Heliyon 8 (2022) e10058

Contents lists available at ScienceDirect

Heliyon

journal homepage: www.cell.com/heliyon

Research article

A wideband circularly polarized CPW-fed substrate integrated waveguide based antenna array for ISM band applications

Sarosh Ahmad [a,b,*], Nabil Cherif [c], Salman Naseer [d], Umer Ijaz [a], Yanal S. Faouri [e], Adnan Ghaffar [f], Mousa Hussein [g,**]

[a] Department of Electrical Engineering and Technology, Government College University Faisalabad (GCUF), 38000, Faisalabad, Pakistan
[b] Department of Signal Theory and Communications, Universidad Carlos III de Madrid, 28911 Leganés, Madrid, Spain
[c] LSTE Laboratory, Mustapha Stambouli University, Mascara, Algeria
[d] Department of Information Technology, University of the Punjab Gujranwala Campus, Pakistan
[e] Electrical Engineering Department, The University of Jordan, Amman, Jordan
[f] Department of Electrical and Electronic Engineering Auckland University of Technology, Auckland, New Zealand
[g] Department of Electrical Engineering, United Arab Emirates University, Al Ain 15551, United Arab Emirates

ARTICLE INFO

Keywords:
ISM band
Wideband
Circular polarization
SIW
CPW
Axial ratio

ABSTRACT

This article presents a compact size circularly polarized substrate integrated waveguide (SIW) based wideband antenna array that serves industrial, scientific, and medical (ISM) band applications. A coplanar waveguide (CPW) technique is used to ensure the antenna size compactness. The proposed antenna is fabricated on a low-profile Rogers RT6002 substrate with a dielectric constant of 2.94, tanδ of 0.0012 and an approximate height of 0.76mm. The proposed design covers the frequency range from 2.15 GHz to 3.63 GHz (60.4%) while the axial ratio has a 3 dB bandwidth covering from 2.19 GHz to 2.51 GHz (13%) at the operating band of 2.45 GHz. The antenna is miniaturized and has a size of about $46.50 \times 29 \times 0.76$ mm^3. The simulation and experimental results are taken into consideration and there is a good promise between them. Hence, the antenna is a suitable applicant to be utilized for the applications in the ISM band.

1. Introduction

Circular polarization is an imperative and suitable feature of wireless communication systems that require the electromagnetic waves to be resilient to fading and polarization mismatch is circular polarization. Circular polarization is a phenomenon where two perpendicular modes with in-phase quadrature and similar amplitude are excited in the same antenna. In planar antennas, this is achieved through inserting perturbations, especially in printed slot antennas [1]. These perturbations include placing L-shaped strips at the corners of the slot, feedline perturbations, different slot shapes. Some of these techniques provide wideband AR bandwidths but a lot suffer from design complexity and difficulty in replication of technique used due to trial and error. In printed monopole antennas, several techniques have also been proposed to generate CP [2].

Sensor nodes with ISM-band antennas are essential for high-quality data transmission in wireless sensor networks. A SIW-based antenna built on a single planar sheet offers the flexibility and simplicity needed to be incorporated into infrared-operated chemical sensors. Researchers have been interested in creating the Substrate-Integrated Waveguide (SIW), a simple technology compatible with planar circuits and easy integration with other components, with features that can increase the performance or packaging of RF circuits in recent years. Rectangular waveguides and microstrip or CPW technology are compatible with SIW technology. Simple PCB manufacturing processes are employed in SIW planar technology, which has been exploited for ISM band applications [3].

Recently, communication system research has centered on lowering weight, reducing size, and boosting dependability at a lower cost. Microwave components such as power dividers, antennas, and filters are critical components in today's telecommunications systems, including embedded satellite systems and telecommunication systems. Rectangular waveguides are one of the most extensively used microwave components, but their large size makes them difficult to manufacture at a low cost and incorporate into planar systems. To address this issue, scientists are

* Corresponding author.
** Corresponding author.
E-mail addresses: saroshahmad@ieee.org (S. Ahmad), mihussein@uaeu.ac.ae (M. Hussein).

https://doi.org/10.1016/j.heliyon.2022.e10058
Received 26 February 2022; Received in revised form 29 March 2022; Accepted 19 July 2022

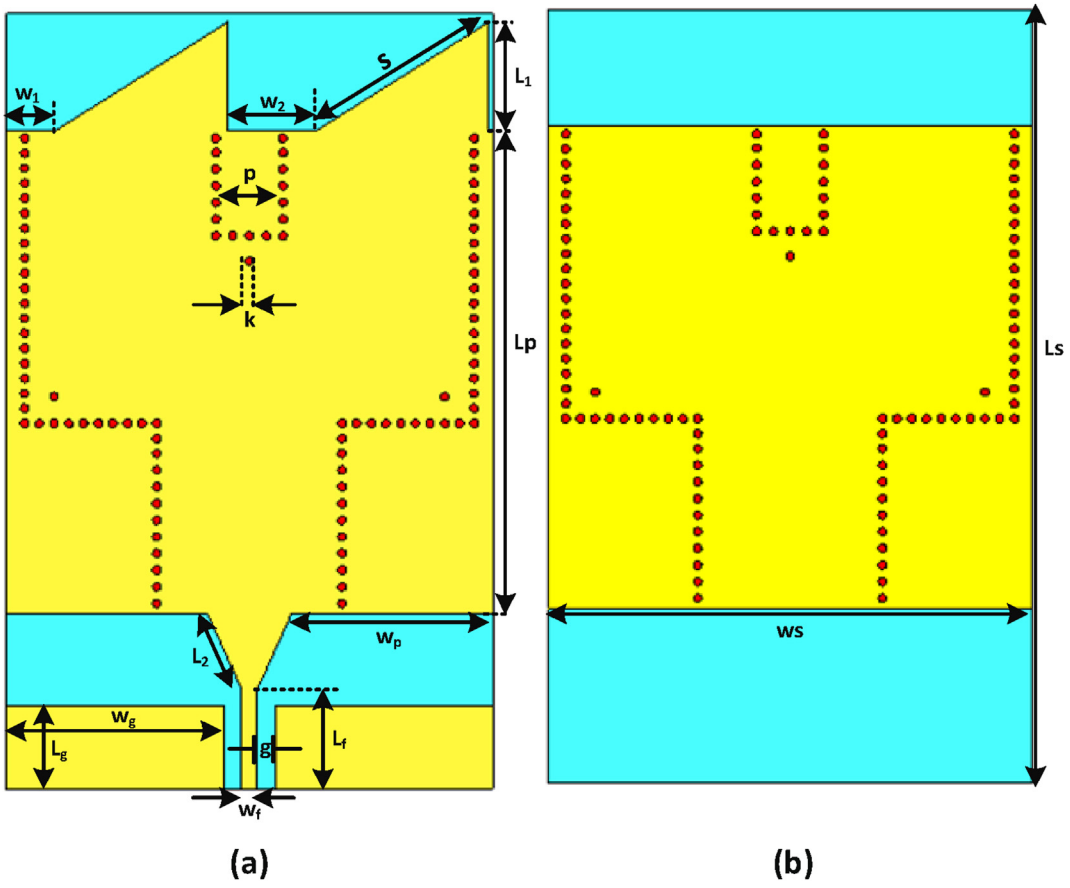

Figure 1. Proposed Antenna's geometry, (a) top view, (b) bottom view.

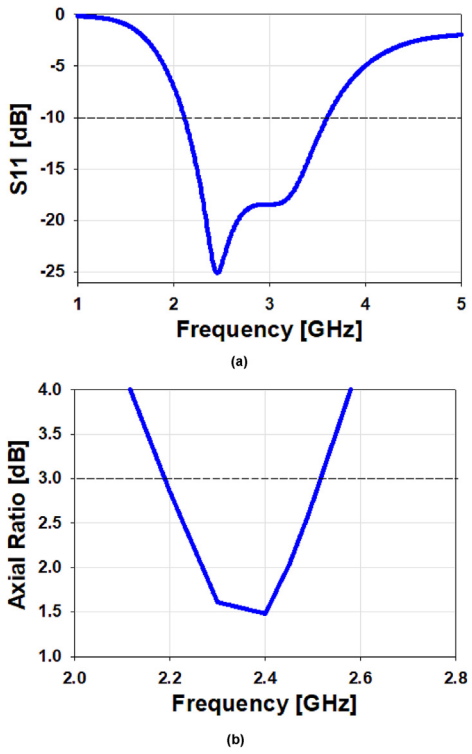

Figure 2. Proposed SIW-based antenna; (a) reflection coefficient [dB], (b) axial ratio [dB].

studying and developing a novel planar structure known as a substrate integrated waveguide (SIW) [4]. A geometrical periodic and aperiodic cell carved on the ground plane of RF integrated circuits is known as the DGS method. The flow of the surface current is disrupted by this defective ground plane, and the current's disorder modifies the structure's properties, as proposed in [5].

By combining two higher-order modes utilizing both bowtie and rectangular-shaped slots; the SIW cavity-backed antenna can cover a wide frequency range. To create the twin slot layout for bandwidth enhancement, a shorting through is added above the rectangular slot. Through reducing the quality factor and therefore increasing bandwidth, modified and unmodified triangular slots are used to create a dual-frequency band of operation. Multiple shorting pins have been merged with SIW cavity-backed antenna in [6] to increase the bandwidth by up to 20% through utilizing beyond two higher-order modes. A high length to width ratio SIW cavity supported antenna with an elliptical-shaped slot has been designed in [7] to increase the antenna's gain through exciting an odd number of modes in TE_{1m0}. Three slots of rectangular shape are separated by a quarter wavelength distance in [8] to boost the antenna's directivity. The ratio of the main lobe to the back lobe and the bandwidth of a SIW cavity-backed aerial with a dielectric resonator are both improved. By improving the irregularly shaped slot, the Particle Swarm Optimization approach is used to boost the covered frequency band of the SIW cavity-backed aerial. In [9], two sloped rectangular slots, as well as shorting pins, are utilized to enhance bandwidth. The circular SIW cavity supported slotted antenna with an enhanced gain is developed to achieve high gain performance [10].

According to the mode of communication, centric communication can be divided into three groups (examined in [11, 12, 13]) (in, off, and on)-body communication. The proposed design is an implantable device

Table 1. Parametric study of the SIW-based proposed antenna in 'mm'.

Constraints	Values	Constraints	Values
L_S	46.5	W_S	29
L_f	6	W_f	0.95
L_1	6.5	W_1	2.95
L_2	4.93	W_2	5.3
Lp	29	Wp	12
G	1.03	S	12.13
K	0.5	P	3.5

with an offender on the human body skin, and the sensors were initially implanted into corporeal body phantasms. On-body correspondence, on the other hand, refers to a situation in which several sensors are linked to the body and require self-communication inside the body area network (BAN). The last strategy, which involves transmitting data from sensors (antennas) to nature through a physical frame, such as a monitoring center or a repair appliance, and, in general, constructing a personal area network between several persons and neighboring gadgets, is the most useful. Fundamentally, under the impact of the physical body, the proposed-efficiency antennas and performance are lessened, and the SAR quantity is dramatically diminished. ISM band antennas for medical applications are becoming increasingly important in enlightening patients' life capacities. The telecommunication strategy using a far-field antenna for radiocommunication between bio-medical implantations and external display gadgets has several advantages over its conservative near-field complement, including high data-rates long-distance communication [14, 15, 16, 17].

This research proposes a circular-shaped ground radiating patch antenna for biomedical implantable applications that operate in the ISM (2.4–2.5 GHz) band. A circular configuration was chosen because it has a similar antenna shape and size to medicinal tablets (pills), and it avoids sharp edges, making it easier to eat and implant. The paper's major focus is on constructing and evaluating a miniaturized antenna construction with acceptable performance for biotelemetry applications. The CP radiation feature is produced by achieving a quadrature-phase difference by inserting asymmetric square slots in the ground regarding the coplanar waveguide (CPW) feed.

A low-profile circularly polarized compact SIW-based antenna array for 2.45 GHz ISM band applications is designed in this research, employing a flexible low-profile Rogers material commercially marketed as Rogers RT6002. The antenna has a 10-dB characteristic impedance bandwidth from 2.1 GHz to 3.63 GHz (60.4%) while the 3 dB axial ratio bandwidth covers from 2.19 GHz to 2.51 GHz (13%). The proposed antenna's dimensions are 46.5 × 29 × 0.76 mm^3, demonstrating its compactness in contrast to current antennas. The bending analysis of the antenna along x-axis and the y-axis are also taken into consideration.

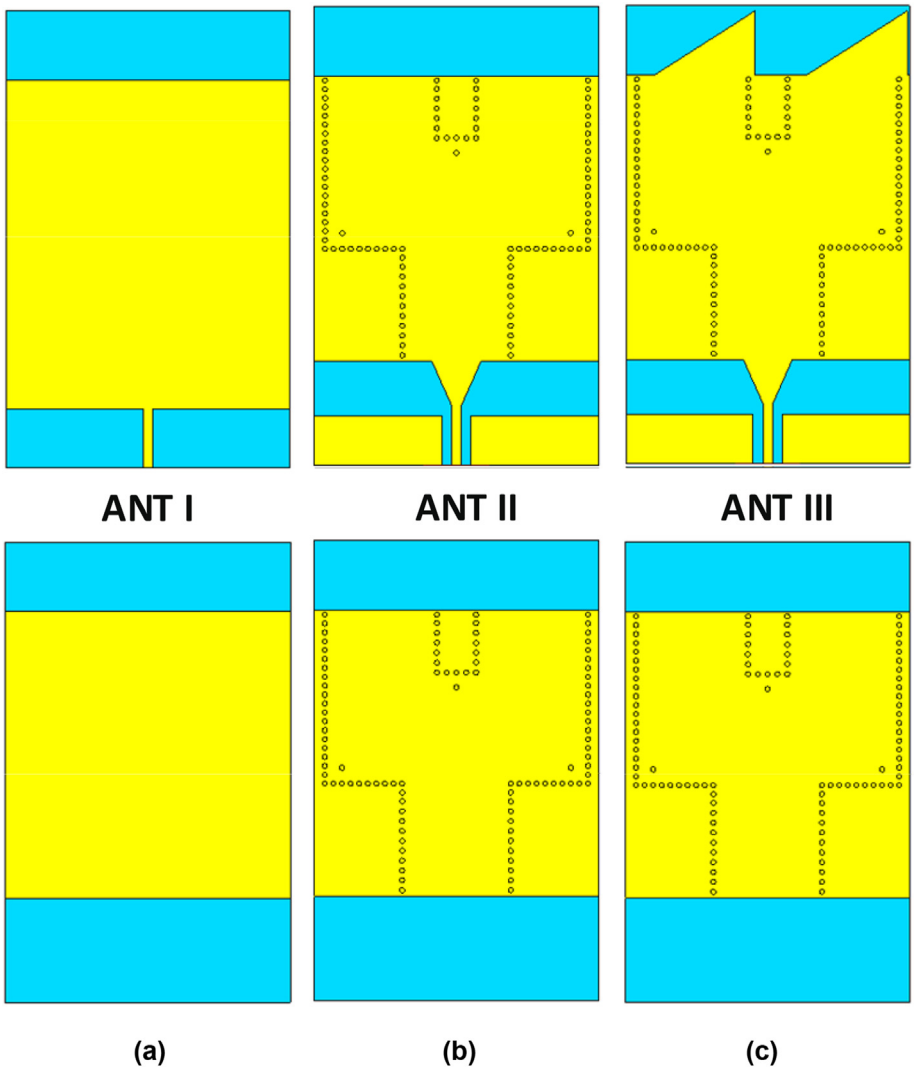

Figure 3. Proposed antenna design steps (a) simple rectangular radiator (ANT I), (b) SIW power divider (ANT II), (c) Proposed antenna array (ANT III).

Designing analysis of the SIW-based antenna is proposed in Section II. Section III summarizes the proposed antenna results and analysis. While the conclusion is proposed in the last section.

2. Design analysis of the antenna

The proposed flexible circularly polarized substrate-integrated waveguide (SIW)-based antenna array is shown in Figure 1 and its S_{11} and axial ratio versus frequency (GHz) graphs are shown in Figure 2. The proposed geometry is made up of three parts: the first is the taper transition for impedance matching between the microstrip and the SIW. The second part is the SIW featured by the Roger 6002 substrate thickness of 'ts = 0.76 mm' and its permittivity relative of '$\varepsilon_r = 2.94$', the diameter of 'k = 0.5 mm' of the metal vias, the distance 'p = 3.5 mm' between centers of two successive via and the transverse spacing '$w_2 = 5.3$ mm' between the centers of opposite vias which is given by the same propagation characteristics with the equivalent waveguide. The third part consists of linearly tapered slot antenna array printed on Rogers RT6002 substrate fed by SIW two-way power divider having T-junction configuration. The overall volume of the antenna is 46.5 × 29 × 0.76 mm^3. Computer simulation technology (CST) microwave studio 2018 is used for simulations and optimizations of the design. Table 1 lists the optimized

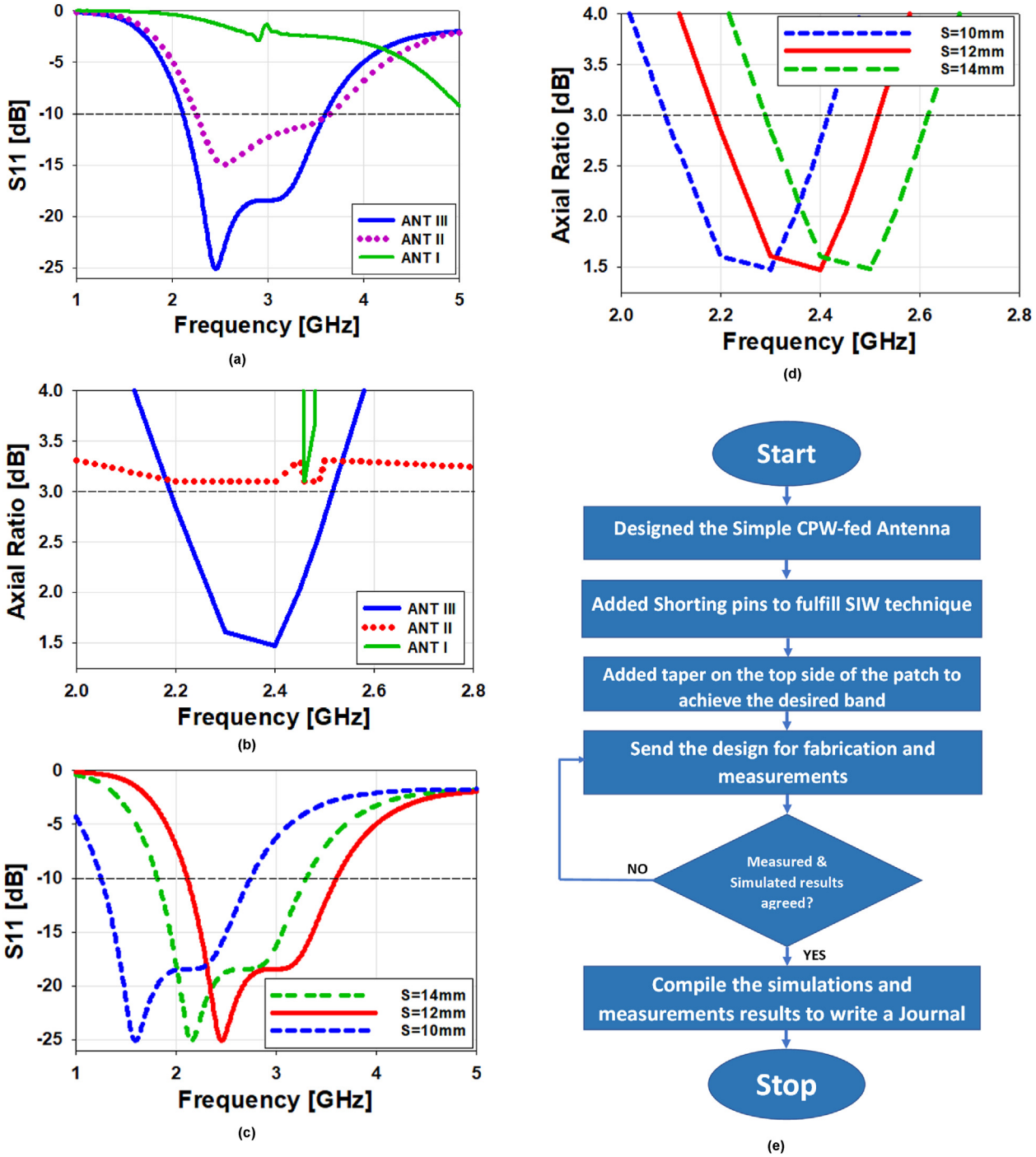

Figure 4. (a) S_{11} comparison for the antenna design steps (b) axial ratio comparison for the antenna design steps, (c) S_{11} comparison for the length of the taper 's', (d) axial ratio comparison for the length of the taper 's'. (e) flowchart for the proposed antenna mechanism.

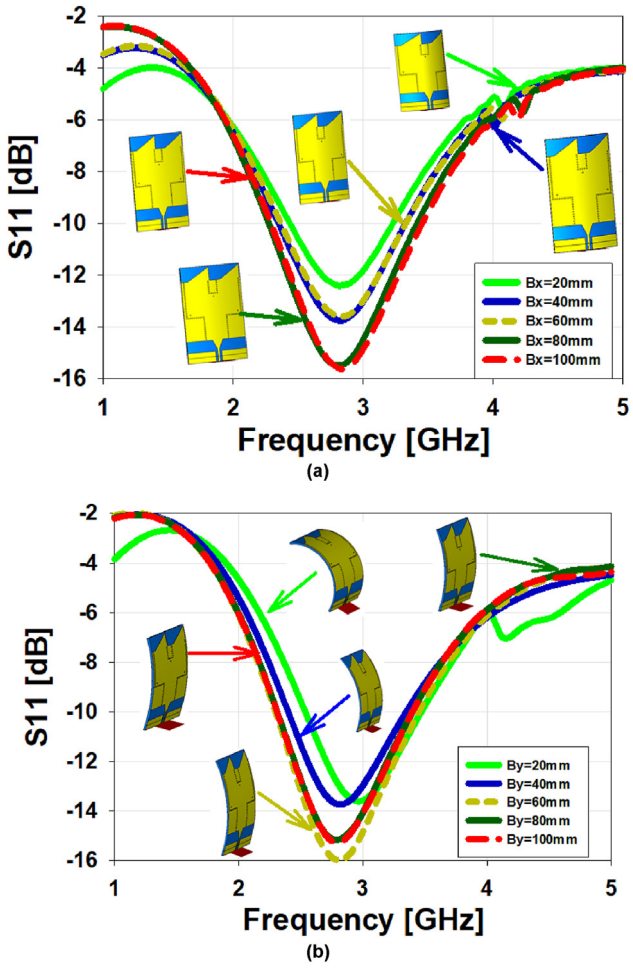

Figure 5. Twisting study of the proposed design; (a) along the x-axis, (b) along the y-axis.

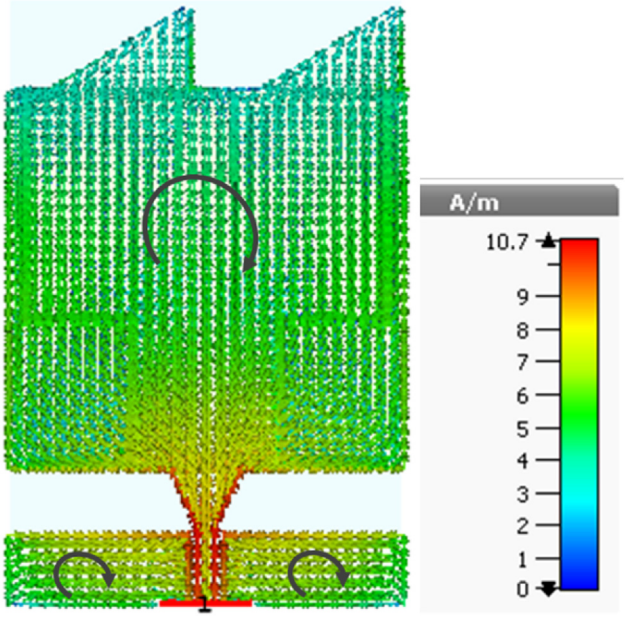

Figure 6. Current distribution at the antenna surface at 2.45 GHz.

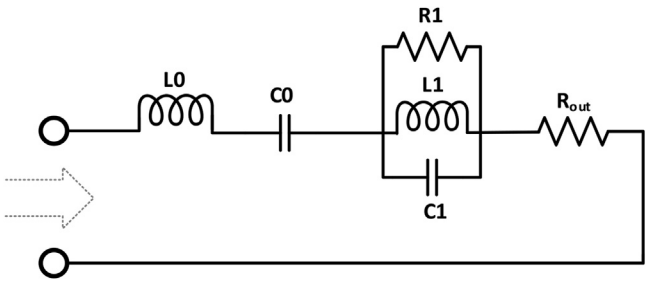

Figure 7. The corresponding circuit schematic for the ISM band antenna.

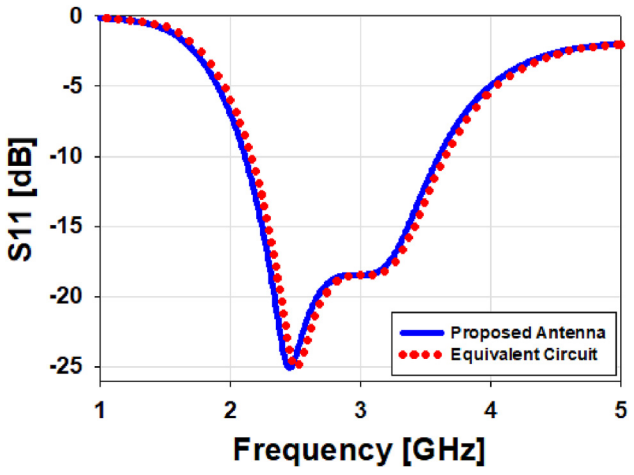

Figure 8. S_{11} [dB] comparison between the proposed antenna and the equivalent circuit prototype.

Table 2. Equivalent circuit components values.

Inductors	Values (nH)	Capacitors	Values (pF)	Resistors	Values (Ω)
L0	15	C0	0.277	R1	75
L1	0.1	C1	3	Rout	50

parameters of the stated design. The most accurate design equation of a SIW is given by Eq. 1 (a-c)

$$a_d = Wsiw\left\{\xi_1 + \frac{\xi_2}{\frac{b}{d} + \frac{\xi_1+\xi_2-\xi_3}{\xi_3-\xi_1}}\right\} \quad (1)$$

Where:

$$\xi_1 = 1.0198 + \frac{0.3465}{\frac{Wsiw}{b} - 1.0684} \quad (1a)$$

$$\xi_2 = -0.1183 - \frac{1.2729}{\frac{Wsiw}{b} - 1.2010} \quad (1b)$$

$$\xi_3 = -0.1183 - \frac{1.2729}{\frac{Wsiw}{b} - 1.2010} \quad (1c)$$

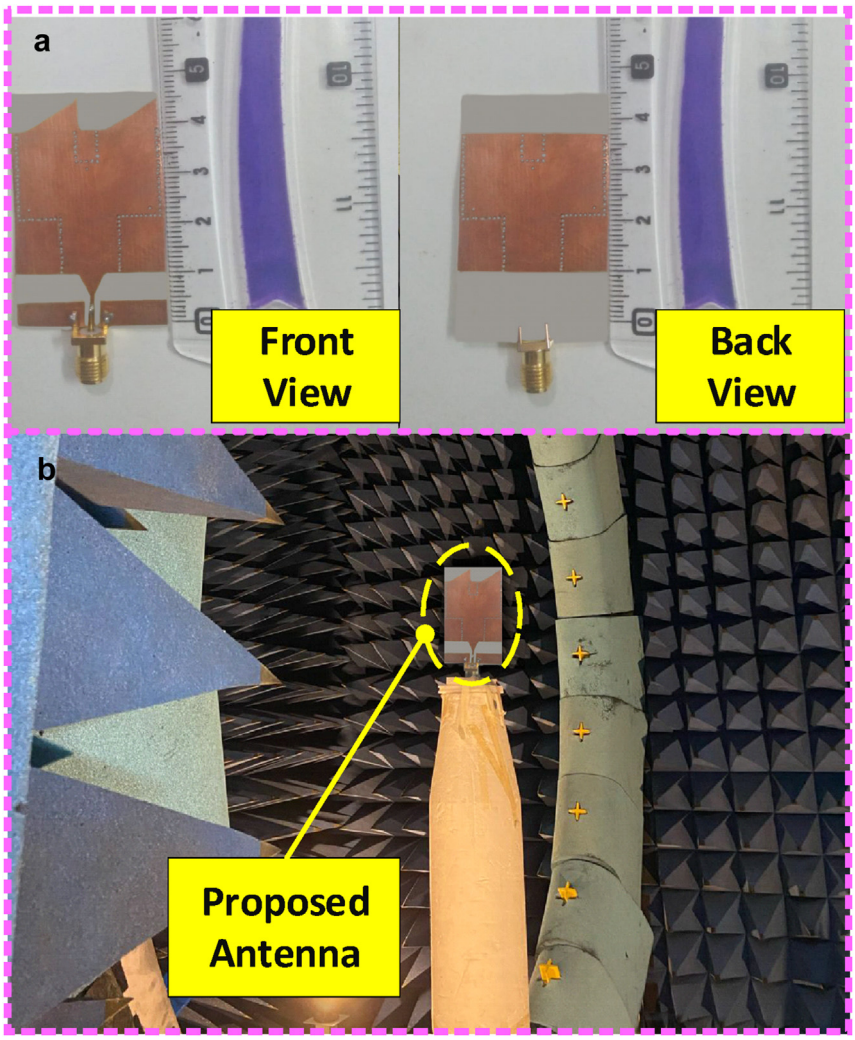

Figure 9. (a) Manufactured antenna (front and back view), (b) Mounted antenna inside an anechoic chamber.

Where d is the diameter of metal vias, b is the distance between two consecutive vias and Wsiw is the width of SIW. For minimizing, the losses two conditions are required.

$d < \lambda g \times 0.20$ and $b \leq 2 \times d$

Where λg is the guided wavelength as given in Eq. (2).

$$\lambda g = \frac{2\pi}{\sqrt{\frac{(2\pi f)^2 \varepsilon_r}{c^2} - \left(\frac{\pi}{a}\right)^2}} \tag{2}$$

The dielectric filled waveguide width "*ad*" is calculated by Eq. (3) where ε_r is the dielectric relative permittivity.

$$a_d = \frac{a}{\sqrt{\varepsilon_r}} \tag{3}$$

The transition between the microstrip and the SIW requires the calculation of the output impedances Zpi from the input impedance, which is equal to 50Ω. The Zpi is given by Eq. (4)

$$Z_{pi} = Z_{TE} \frac{\pi^2 h}{8 Wsiw} \tag{4}$$

Z_{TE}: represent the wave impedance for the TE_{10} mode it's given by Eq. (5).

$$Z_{TE} = j\omega \frac{\mu'}{\beta} = \sqrt{\frac{\mu}{\varepsilon_r}} \times \frac{\lambda_g}{\lambda} \tag{5}$$

Rogers's 6002 substrate is a low loss and low dielectric constant laminate to provide high electrical and mechanical properties essential in designing of microwave structures. In our design, we used Rogers 6002 which is characterized by a loss tangent of about 0.0012, a dielectric constant of 2.94 and the thickness of 0.76 mm. The features of this substrate are:

- Low Loss
- Suitable for high frequency performance
- Excellent electrical properties
- Suitable for applications sensitive to Temperature change
- Excellent dimensional stability

2.1. Proposed antenna design steps

First, Figure 3 demonstrates a basic rectangular microstrip antenna (ANT I) with a feedline is designed. The response of the S_{11} and the axial ratio for the antenna design steps are shown in Figure 4 (a & b). With ANT I, the antenna didn't show any performance and there is no circular polarization achieved. Then in the second step (ANT II), a SIW-based technique is used to achieve the band of the antenna at 2.45 GHz but

still, there is no circular polarization behavior. Then in the third step (ANT III), there is an integration between the power divider and the antenna elements to construct a 1 × 2 linear antenna array operates at 2.4 GHz with a reflection coefficient less than -10 dB at the anticipated operating band of 2.45 GHz and the circular polarized has been attained with this third step with 3dB axial ratio bandwidth of 13% as depicted in Figure 4. Parametric study of the important parameter 'S' of the proposed design is taken into consideration that helps to clarify the S_{11} behavior and the AR behavior of the antenna as shown in Figure 4 (c & d). The value of the taper length 's' is varied from 10mm to 14mm, and it is noticed that the frequency is also shifted towards lower frequency band and the axial ratio is also shifted towards the lower frequency band by decreasing the length of the taper and shifted to the higher band by increasing the length of the taper. The proposed antenna design flow-chart is shown in Figure 4 (e).

2.2. Bending analysis of the antenna

The antenna's conformability and stretchiness are demonstrated by bending analysis. The antenna has been used for ISM band applications since then. As a result, the antenna's bending behavior must be investigated. To analyze the S_{11} behavior, gain, and far-field of the antenna, several twisting radii (Bx = By = 20 mm–100 mm) are chosen along the x- and y-axes. In Figure 5, the antenna's simulated results when bent along the x- and y-axes are compared. It is commonly known that all twisting radii contain needless modifications. Figure 5(a) indicates the comparison between different bending radii along the x-axis. While Figure 5(b) shows the comparison of the bending radii along the y-axis. An antenna's surface current density reveals which region of the antenna

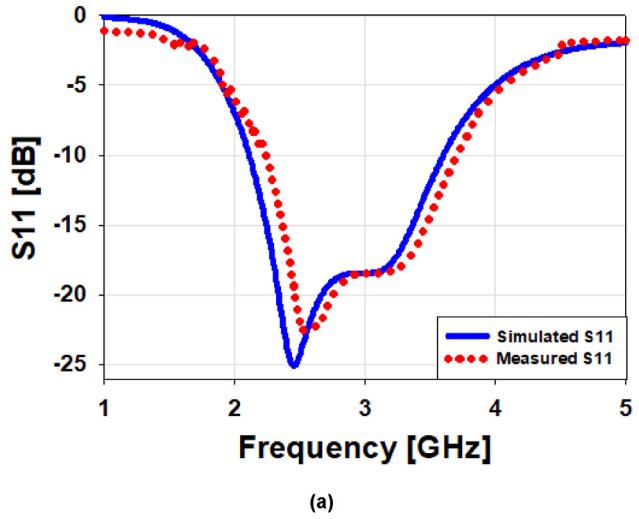

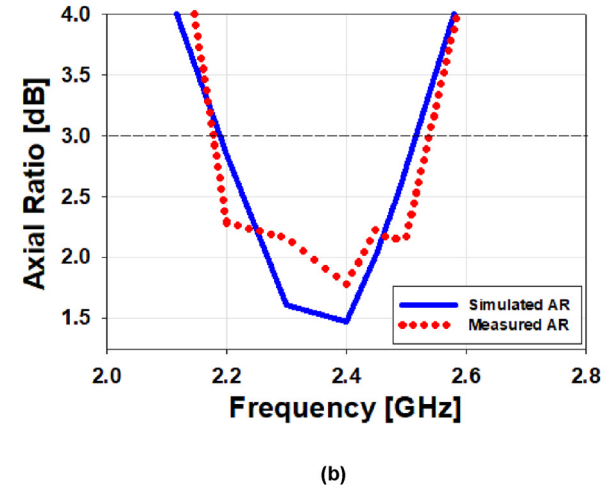

Figure 10. Comparison between the simulated and measured S_{11} and axial ratio in Free Space.

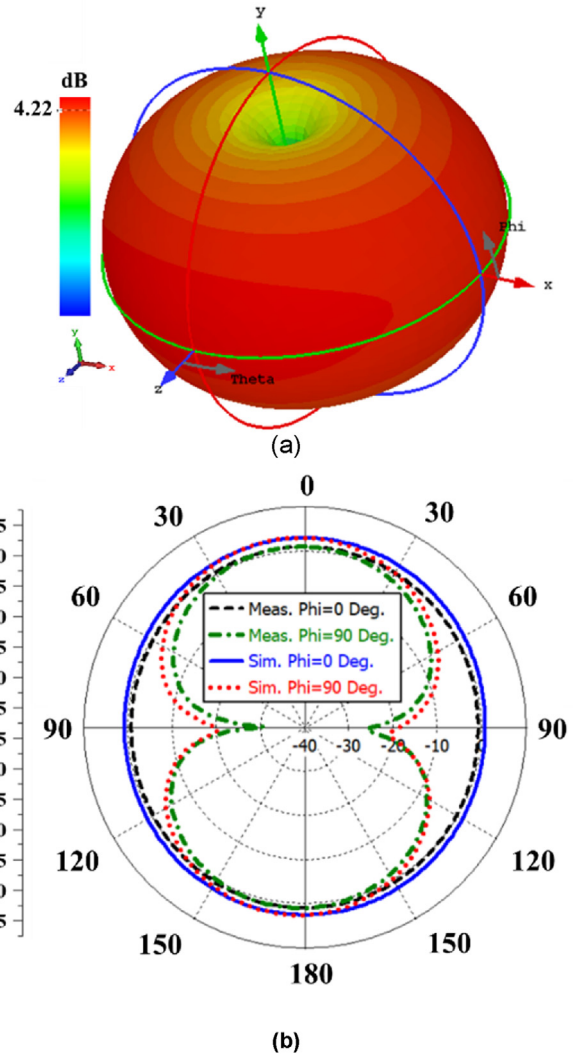

Figure 11. (a) 3D radiation pattern, (b) 2D-Pattern of the antenna at 2.45 GHz.

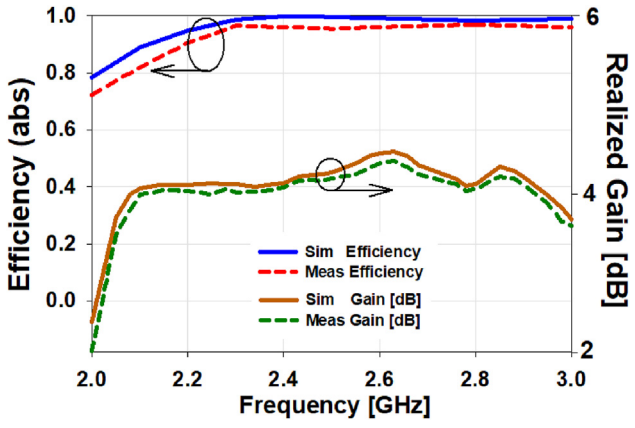

Figure 12. In free space, the simulated and observed S_{11} and axial ratios are compared.

Table 3. Comparison of antenna's Performance for different on/off body.

Ref.	Dimensions (mm^3)	Substrate Material	Imp BW (%)	Gain (dBi)
[18]	50 × 50×0.6	FR-4	<10.5	1.2/7.9
[19]	100 × 100×2	Felt	<11.9	6.33/6.98
[20]	100 × 30×3.6	Leather	<23.1	5.10/3.3
[21]	30.5 × 62×3.15	Taconic TLY	<3.47	1.51/6.44
[22]	30 × 45×3.2	FR-4	<4.9	3.09/0.64
[23]	58 × 40 × 0.8	FR-4	>65	3.2
[This work]	46.50 × 29×0.76	RT6002	65.4	>4.2

is important in getting it to resonate at the appropriate frequency. Figure 6 shows the surface current density at 2.45 GHz. The feedline and the upper section of the patch have the dominant effect in creating a resonance at 2.45 GHz. In simple words, the surface current distribution provides the great insight regarding mode of propagation.

2.3. Equivalent electrical circuit prototype

The proposed electrical circuit prototype is constructed using an advanced design system (ADS) simulator, as shown in Figure 7, and the circuit response is also shown in Figure 8. To mimic the antenna input impedance and operation in the single band, the proposed model uses parallel RLC circuits connected to a capacitor 'C0', inductor 'L0' and resistor 'R_{out}' in series. Table 2 summarizes the equivalent circuit components values.

To obtain operation at 2.45 GHz, an RLC circuit relates to a capacitor and an inductor. We can enhance the S_{11} of the equivalent circuit by changing the values of the resistors while varying inductors and capacitors can change the operating band. Figure 8 shows a comparison of the circuit model's simulation results and the proposed antenna's simulation results.

3. Fabrication and measurements

Figure 9 depicts the built prototype on an FR-4 substrate, whereas Figure 10 depicts the S_{11} measurement. As shown in the figures, the measured $|S_{11}|$ [dB] is similar to the modelled $|S_{11}|$ [dB]. In computations, the provided antenna can cover a frequency range (2.15–3.63) GHz with a percentage bandwidth (PBW) of 60.4% at 2.45 GHz, whereas in measurements, the covered frequency range is from 2.25 GHz to 3.67 (59%) GHz (60.4%) at 2.45 GHz, as illustrated in Figure 10. The bandwidth covered by the simulated and observed 3dB axial ratios is from 2.19 GHz to 2.51 GHz (13%) and from 2.2 GHz to 2.49 GHz (11.8%), respectively.

The *E*-plane (Phi = 90) and *H*-plane (Phi = 0) of the simulated and observed radiation pattern in free space are shown in Figure 11. In *E*-plane (Phi = 90), the stated antenna has shown an elliptical radiation pattern while the omnidirectional radiation pattern in *H*-plane (Phi = 0). The antenna's simulated and measured peak gains are 4.35 dB and 4.22 dB at 2.45 GHz, respectively, whereas the simulated efficiency is 99% and the measured efficiency is 97% at the frequency of the ISM band as can be seen in Figure 12. The comparison of the results with similar designs reported in the literature is tabulated in Table 3.

4. Conclusion

A flexible SIW-based antenna array for industrial, scientific, and medical (ISM) spectrum applications is presented and discussed. The proposed antenna tends to have an elliptical in the E-plane and omnidirectional in the H-plane at 2.45 GHz. The flexible roger material RT6002 is utilized, which has a standard height of 0.76 mm and a dielectric constant of 2.3. The twisting analysis along the x- and y-axes is also considered due to the flexible substrate. The proposed antenna has a measured impedance of around 59% and a 3dB axial ratio bandwidth of roughly 11.8%. As a result, the indicated design is a good candidate for ISM band applications.

Declarations

Author contribution statement

Sarosh Ahmad: Conceived and designed the experiments; Analyzed and interpreted the data; Wrote the paper.

Nabil Cherif: Performed the experiments; Analyzed and interpreted the data; Wrote the paper.

Salman Naseer: Conceived and designed the experiments; Analyzed and interpreted the data; Wrote the paper.

Umer Ijaz: Analyzed and interpreted the data; Contributed reagents, materials, analysis tools or data; Wrote the paper.

Yanal Fouri: Performed the experiments; Wrote the paper.

Adnan Ghaffar: Analyzed and interpreted the data; Wrote the paper.

Mousa Hussein: Contributed reagents, materials, analysis tools or data; Wrote the paper.

Funding statement

This research did not receive any specific grant from funding agencies in the public, commercial, or not-for-profit sectors.

Data availability statement

The authors do not have permission to share data.

Declaration of interest's statement

The authors declare no conflict of interest.

Additional information

No additional information is available for this paper.

References

[1] V.K. Gupta, D. Thakur, Design and performance analysis of a CPW-fed circularly polarized implantable antenna for 2.45 GHz ISM band, Microw. Opt. Technol. Lett. 62 (12) (2020) 3952–3959.

[2] D. Chaturvedi, SIW cavity-backed 24° inclined-slots antenna for ISM band application, Int. J. RF Microw. Computer-Aided Eng. 30 (5) (2020) e22160.

[3] A. Birwal, V. Kaushal, K. Patel, Circularly polarized broadband Co-planar waveguide fed antenna for 2.45 GHz RFID reader, IEEE Int. Conf. RFID Tech. App. (RFID-TA) (2021) 109–112.

[4] A. Iqbal, J.J. Tiang, S.K. Wong, S.W. Wong, N.K. Mallat, SIW cavity-backed self-quadruplexing antenna for compact RF front ends, IEEE Antenn. Wireless Propag. Lett. 20 (4) (April 2021) 562–566.

[5] M. V, N. D. M, J. M, Design and Performance Analysis of SIW Cavity-Backed Sectored Slot Antenna for ISM Band Applications," 2021 Sixth International Conference on Wireless Communications, Signal Processing and Networking (WiSPNET), 2021, pp. 126–129.

[6] R.S. Raghav, T.M.B. Shankar Balu, A. Shwetha, K. Aravinth, M. Vamshi, V. Mekaladevi, SIW Cavity-Backed Self-Diplexing T-Shaped Slot Antenna", Electronics and Sustainable Communication Systems (ICESC) 2021 Second International Conference on, 2021, pp. 616–619.

[7] S. Mukherjee, A. Biswas, Design of planar high-gain antenna using SIW cavity hybrid mode, IEEE Trans. Antenn. Propag. 66 (2) (2017) 972–977.

[8] Aparna Ajith R, K S Ajith Bhaskar, Harihara P. Prasaad, V. Mekaladevi, SIW Cavity-Backed Pentagonal Slot Antenna for X-Band Applications", Computing Communication and Networking Technologies (ICCCNT) 2021 12th International Conference on, 2021, pp. 1–4.

[9] Han-Yu Xie, Bian Wu, Yue-Lin Wang, Chi Fan, Jian-Zhong Chen, Tao Su, Wideband SIW filtering antenna with controllable radiation nulls using dual-mode cavities, Antenn. Wireless Propag. Let. IEEE 20 (9) (2021) 1799–1803.

[10] M. Rizal, N. Ismail, K.A. Munastha, A. Munir, "SIW-based Radial-Line-Slot-Array Antenna for Wireless Communication," 2020 14th International Conference on Telecommunication Systems, Services, and Applications (TSSA), 2020, pp. 1–4.

[11] P. Sambandam, M. Kanagasabai, R. Natarajan, M.G.N. Alsath, S. Palaniswamy, Miniaturized button-like WBAN antenna for off-body communication, IEEE Trans. Antenn. Propag. 68 (7) (July 2020) 5228–5235.

[12] Yeboah-Akowuah Bright, Eric Tutu Tchao, Masood Ur-rehman, Mohammad Monirujjaman Khan, Sarosh Ahmad, study of a printed split-ring monopole for dual-spectrum communications, Heliyon 7 (9) (2021) e07928.
[13] M.A. Shahzad, K.N. Paracha, S. Naseer, S. Ahmad, M. Malik, M. Farhan, A. Ghaffar, M. Hussien, A.B. Sharif, An artificial magnetic Conductor−Backed compact wearable antenna for smart watch IoT applications, Electronics 10 (2021) 2908.
[14] S. Ahmad, et al., A metasurface-based single-layered compact AMC-backed dual-band Antenna for off-body IoT devices, IEEE Access 9 (2021) 159598–159615.
[15] A. Ghaffar, W.A. Awan, N. Hussain, S. Ahmad, X.J. Li, A Compact SIW-Based Flexible Antenna for Applications at 900 and 2450 MHz," Progress in Electromagnetic Research, PIER), 2021.
[16] Sarosh Ahmad, Adnan Ghaffar, Niamat Hussain, Nam Kim, Compact dual-band Antenna with paired L-shape slots for on- and off-body wireless communication, Sensors 21 (23) (2021) 7953.
[17] Yawar Ali Sheikh, Kashif Nisar Paracha, Sarosh Ahmad, Abdul Rauf Bhatti, Arslan Dawood Butt, Sharul Kamal Abdul Rahim, Analysis of the compact CP/LP Patch antenna design for wearable application, Arabian J. Sci. Eng. (2021).
[18] C. Zhao, W. Geyi, Design of a dual-band dual mode antenna for on/off-body communications, Microw. Opt. Technol. Lett. 62 (2019) 514–520.
[19] T.T. Zhou, S.J. Fang, X. Jia, Dual-band and dual-polarised circular patch textile antenna for on/off-body WBAN applications, IET Microw., Antenn. Propag. 14 (2020) 1751–8725.
[20] R. Pei, M.P. Leach, E.G. Lim, Z. Wang, C.Y. Song, J.C. Wang, W.Z. Zhang, Z.Z. Jiang, Y. Huang, Wearable EBG-backed belt antenna for smart on-body applications, IEEE Trans. Ind. Inf. 16 (2020) 7177–7189.
[21] Y. Hong, J. Tak, J. Choi, Dual-band dual-mode patch antenna for on–on–off WBAN applications, Electron. Lett. 50 (2014) 1895–1896.
[22] J. Tak, S. Woo, J. Kwon, J. Choi, Dual-band dual-mode patch antenna for on-/off-body WBAN communications, IEEE Antenn. Wireless Propag. Lett. 15 (2016) 348–351.
[23] Boddapati T.P. Madhav, Shaik Rajiya, Badugu P. Nadh, Munuswami S. Kumar, Frequency reconfigurable monopole antenna with DGS for ISM band applications, J. Elect. Eng. 69 (No 4) (2018) 293–299.